Weather Clim. Dynam., 6, 265–277, 2025
https://doi.org/10.5194/wcd-6-265-2025

Weather and Climate Dynamics
Open Access
EGU

Atmospheric mixed Rossby–gravity waves over the tropical Pacific during the austral summer

Hugo A. Braga and Victor Magaña

Departamento de Geografía Física, Instituto de Geografía, Universidad Nacional Autónoma de México, 04510, Mexico City, Mexico

Correspondence: Hugo A. Braga (hugoalvesbraga@icloud.com)

Received: 23 October 2024 – Discussion started: 5 November 2024
Revised: 10 January 2025 – Accepted: 12 January 2025 – Published: 5 March 2025

Abstract. Atmospheric mixed Rossby–gravity wave (MRGW) activity during the austral summer months (December–January–February) is examined by means of observational analyses for the 1991–2020 period. The main objective of the study is to explore the relationship between tropical circulations at upper- and lower-tropospheric levels and tropical convective activity. Using an empirical orthogonal function (EOF) analysis of the high-frequency meridional component anomalies of the wind at 200 hPa, for zonal wavenumbers 4–6, episodes of intense MRGW activity are detected. Composite analyses based on an EOF analysis show a quadrature phase over the central eastern equatorial Pacific between the MRGW structure in the upper and lower troposphere. Lagged correlations between the first two EOFs' principal components, as well as the wind field and outgoing longwave radiation (OLR), show that MRGWs are laterally forced at upper-tropospheric levels over the westerly duct region and later propagate westward and downward. Once the MRGW reaches the lower-tropospheric levels, it induces zones of moisture convergence that modulate convective activity. Tropical convection develops in the MRGW moisture convergence region at 700 hPa and the divergent region of the wave at 200 hPa. Since the MRGW phase tilts eastward with height, moisture convergence at lower-tropospheric levels tends to coincide with divergence at upper levels favoring intense convective activity which results in the antisymmetric outgoing longwave radiation anomalies observed off the Equator near the MRGW. Therefore, the occurrence of MRGWs over the eastern Pacific is a form of tropical–extratropical interaction that generates tropical convection anomalies by means of induced lower-tropospheric moisture convergence and divergence anomalies.

1 Introduction

Equatorial waves are important elements of the atmospheric tropical circulations. Matsuno (1966) determined the main spatial and temporal characteristics of mixed Rossby–gravity waves (MRGWs), later identified by means of observational analyses by Yanai and Maruyama (1966) and Maruyama (1967). In the present study, MRGWs will refer to the westward-moving waves in the troposphere, coupled with tropical convection, like those discussed by Magaña and Yanai (1995). Various observational studies show that MRGWs exhibit fluctuations in the meridional component of the wind, with periods between 4 and 6 d and zonal wave numbers 4 to 6 (Yanai and Hayashi, 1969; Yanai and Murakami, 1970a, b; Nitta, 1970). Their vertical wavelengths range between 6 and 10 km (Holton, 1979; Magaña and Yanai, 1995) with an upward propagation from the upper troposphere to lower-stratospheric levels (Yanai and Hayashi, 1969).

The origin of MRGWs indicates that lateral forcing is a common trigger of MRGWs, as originally proposed in model studies by Mak (1969) and later explored by Bennet and Young (1971), Hayashi and Golder (1978), and Zhang and Webster (1992), among others. Observationally, Yanai and Lu (1983), Magaña and Yanai (1995), Yang and Hoskins (2016), Kiladis et al. (2016), Yang et al. (2018), Suhas et al. (2020), and Shreya and Suhas (2024) also documented MRGWs triggered by lateral forcing. On the other hand,

tropical convective heating has also been suggested as a mechanism that results in MRGWs (Holton, 1972; Hess et al., 1993). Hayashi (1970) proposed that MRGWs could be the result of wave-CISK (conditional instability of the second kind), i.e., by means of the interaction between convective heating and the wave itself. However, Takayabu and Nitta (1993) ruled out wave-CISK as a mechanism to maintain MRGWs. In any event, the relationship between MRGWs and tropical convective activity exists (e.g., Magaña and Yanai, 1995; Kiladis et al., 2009), but a definite answer as to how it works has not been given.

The first observational studies on the vertical structure of MRGWs indicate that they extend from the troposphere to the lower stratosphere (Yanai and Hayashi, 1969). A vertical node of these equatorial waves appears in the upper-tropospheric level (around 200 hPa), and the phase tilts westward to lower-tropospheric levels and eastward into the stratosphere (Magaña and Yanai, 1995; Zhou and Wang, 2007; Kiladis et al., 2009). The tilting of MRGWs plays a crucial role in the vertical transport of momentum and energy (Holton, 1979), but it may also be important in the spatial distribution of the convective activity anomalies associated with MRGWs (Kiladis et al., 2009).

The triggering of MRGWs by midlatitude disturbances from the winter hemisphere takes place in the eastern Pacific westerly duct (Webster and Holton, 1982), which tends to remain "open" in the upper troposphere during the austral summer months (December–January–February) (Braga et al., 2022). During the boreal summer (June–July–August) the westerly duct forms periodically as the Madden–Julian oscillation propagates along the eastern tropical Pacific, which allows the formation of MRGWs (Magaña and Yanai, 1991). Therefore, it is expected that MRGWs triggered by lateral forcing will be more frequent during the austral summer. Their signal at lower atmospheric levels though may be more evident in the region of westerlies, close to the western Pacific (Au-Yeung and Tam, 2018). Consequently, we will focus on this temporal period to examine the relationship between MRGWs triggered in the upper troposphere that extend the signal to lower-tropospheric levels in relation to the development of tropical convection.

A study by Zhou and Wang (2007) shows that an upper-tropospheric MRGW acts as the precursor to a western Pacific tropical depression. Consequently, the downward phase propagation and the vertical structure of the MRGW should be considered in the development of a region of intense convective activity around the equatorial wave. These analyses suggest that an upper-tropospheric MRGW may be reflected in the modulation of moisture convergence and divergence near the boundary layer, which ultimately controls deep convective activity in the equatorial regions. Consequently, the existence of MRGWs and the corresponding antisymmetric anomalies in convective activity (Kiladis et al., 2009) may be considered part of the evolution of MRGWs from upper- to lower-tropospheric levels.

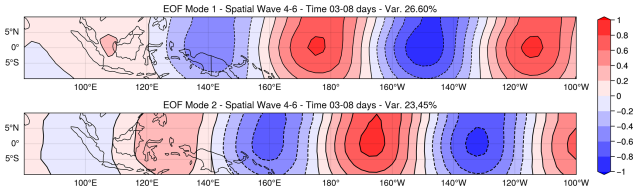

Figure 1. First and second EOF for the 200 hPa space–time-filtered anomaly of the meridional component of the wind field at 200 hPa for December to February of the 1991 to 2020 period.

The present study aims at examining the characteristics and evolution of MRGWs in the Pacific region and the relationship between this type of equatorial wave and convective activity off the Equator, which remains an open scientific question. This study is structured as follows: Sect. 2 outlines the characteristics of the data used for the study and the methodology of investigation. In Sect. 3, observational analyses are developed to determine the characteristics and evolution of MRGWs and their relationship with convective activity. In Sect. 4 the summary and conclusions are presented.

2 Data

2.1 Datasets

For the identification of MRGWs, global reanalyses of ERA5 daily tropospheric winds and specific humidity for the period 1991 to 2020 (Hersbach et al., 2020) have been used. The spatial resolution of ERA5 wind data is 2.5° × 2.5° from 1000 to 100 hPa. Daily outgoing longwave radiation (OLR) data from the National Oceanic and Atmospheric Administration (NOAA) for the same period were also used (Liebmann and Smith, 1996) to document tropical convective activity anomalies.

2.2 Vertically integrated moisture flux

The vertically integrated moisture flux field and its divergence were calculated to evaluate how atmospheric moisture is distributed by tropical disturbances in the tropical regions. The vertically integrated moisture flux (VIMF) is a measure of the amount of water vapor transported in the atmosphere. Its convergence is used in the evaluation of the hydrological processes in the atmosphere (Fasullo and Webster, 2003). High VIMF convergence (VIMFc) zones are related to intense convective activity. The VIMF has been used to examine moisture transport processes, for instance in easterly waves (Pazos et al., 2023). The VIMF is calculated using the expression

$$\mathrm{VIMF} = \frac{1}{g} \int_{p=1000}^{p=100} Vq \, \mathrm{d}p, \tag{1}$$

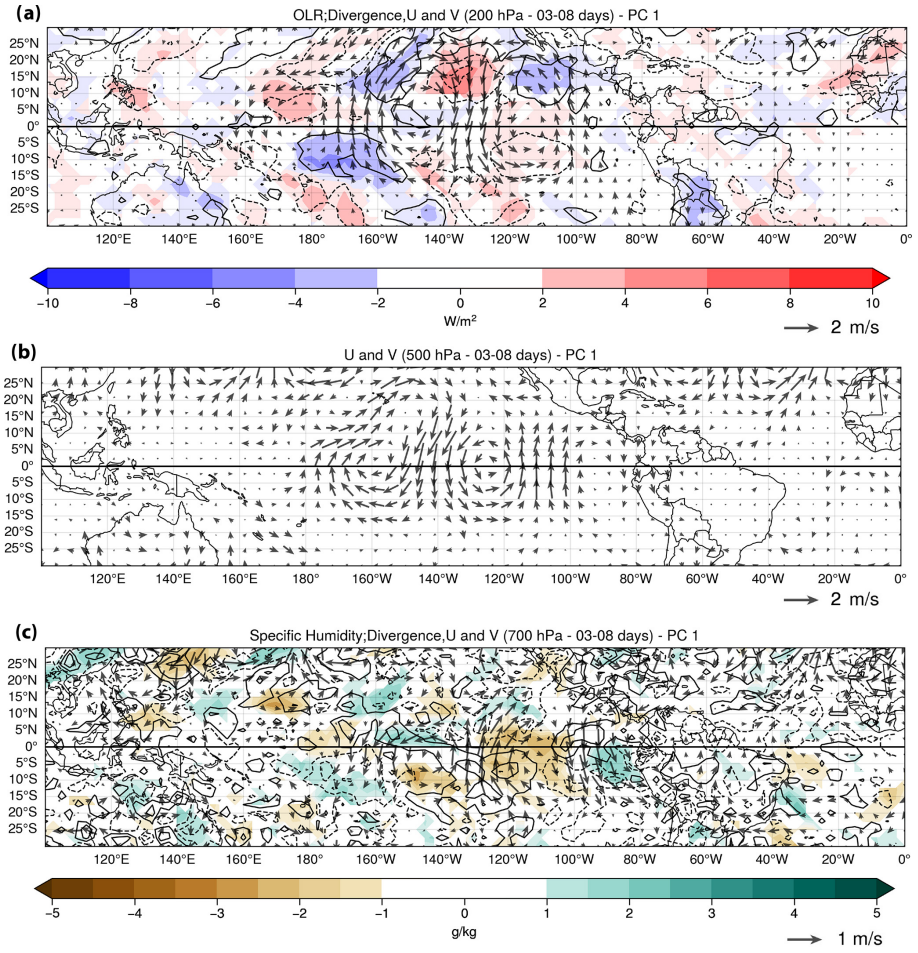

Figure 2. Composite patterns based on PC1 > 1 conditions, showing bandpass-filtered wind anomalies (3–8 d periods) at **(a)** 200 hPa, **(b)** 500 hPa, and **(c)** 700 hPa. Wind anomalies are depicted as vectors, with dashed lines indicating convergence and solid lines showing divergence. Shading represents bandpass-filtered anomalies of outgoing longwave radiation (OLR) (red and blue) and bandpass-filtered specific humidity (brown and green).

where q is the specific humidity (kg kg^{-1}), V is the horizontal wind field, g is the gravity constant, and p is the pressure between 1000 and 100 hPa. VIMF units are kilograms per meter per second (kg m^{-1} s^{-1}).

2.3 Methodology

Various approaches have been used to diagnose MRGW activity including spectral analysis with radiosonde data (Yanai and Hayashi, 1969), reanalysis data (Yanai and Lu, 1983; Magaña and Yanai, 1995; Wheeler and Kiladis, 1999), and by projecting meteorological wind fields of reanalysis data onto the theoretical spatial structures of equatorial waves (Yang et al., 2003; Au-Yeung and Tam, 2018; Knippertz et al., 2022). In this study, MRGW patterns have been identified by means of empirical orthogonal function (EOF) analyses (Kiladis et al., 2016) of the meridional component of the 200 hPa wind field, based on the covariance matrix. Principal components 1 and 2 (PC1, PC2) of EOFs are used as indices to compose wind, OLR, and atmospheric moisture fields to obtain the spatial characteristics of the MRGWs. PC1 and PC2 do not include variations with periods longer than 90 d, which may appear as interannual variations, resulting in the use of data for the December–January–February period. The identification of periods and regions of MRGW activity is determined based on periods of large signals of PC1 or PC2. The temporal evolution of MRGWs is examined by means of lagged correlations between PC1 or PC2 and the wind, OLR, and moisture fields. Data are bandpass-filtered with a Lanczos filter (Duchon, 1979) in the period range between 3 and 8 d. The spatial structure of the MRGW in the EOF analysis is captured with a spatial filter for zonal wavenumbers 4 to 6 (Hayashi, 1982). The wavelength spectrum for the EOFs is limited to the spatial scales characteristic of MRGWs. The inclusion of larger or smaller zonal wavenumbers may capture other modes present in the tropics. However, the main

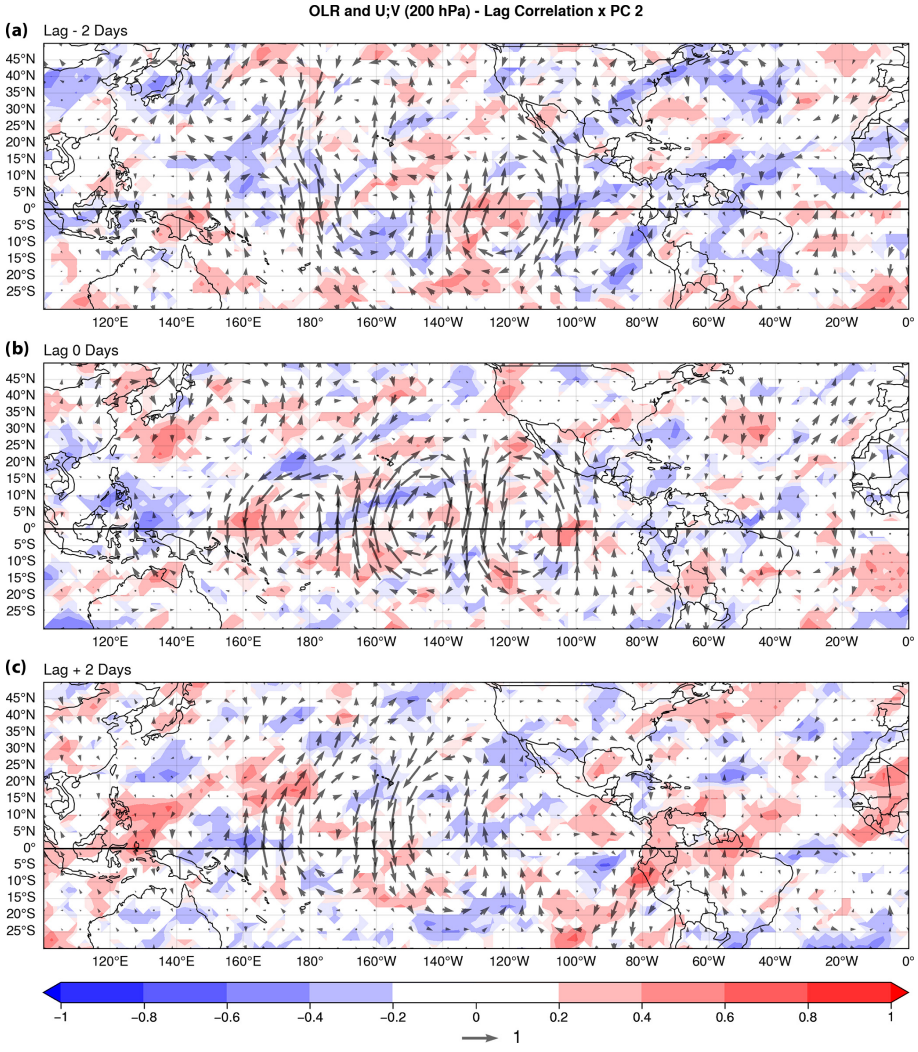

Figure 3. Lagged cross correlation between the PC2 and the wind field anomalies at 200 hPa (vectors) and OLR anomalies (shades of red and blue) for the December–February period. Panels show results for **(a)** lag $= -2$ d, **(b)** lag $= 0$ d, and **(c)** lag $= +2$ d. The correlations are calculated with unfiltered anomalies. A vector of magnitude 1 implies a perfect correlation.

focus of this is on a prototype MRGW with zonal wavenumbers 4–6.

3 Results and discussions

3.1 MRGW detection

The first EOF of the bandpass-filtered component of the meridional wind (v) at 200 hPa, spatially filtered in the 4 and 6 zonal wavenumber range, in the 10° N–10° S, 80° E–100° W domain, similar to the one used by Kiladis et al. (2016) and Suhas et al. (2020), shows the signal of an MRGW with a dominant zonal wavenumber 5 (Fig. 1). EOF2 (EOF mode 2) also captures the MRGW signal, but it is in quadrature with EOF1 (EOF mode 1) (PC2 leads PC1 by approximately 100°), which corresponds to the westward propagation of the wave. The coherence squared between PC1 and PC2 in the 5 to 8 d period range is around 0.66.

To obtain the spatial structure of the wind field corresponding to an MRGW, composite patterns of the space–time bandpass-filtered wind fields at 200, 500, and 700 hPa were constructed using PC1 values larger than 1.0. The composite of the wind field was combined with OLR anomalies at upper levels and specific humidity anomalies at lower levels to obtain the regions of the induced tropical convective activity (Fig. 2). Over the central eastern Pacific, clockwise and counterclockwise circulations, centered along the Equator, show the anomalous wind field of an MRGW (Fig. 2a). In agreement with the theoretical model, its convergent and divergent regions are antisymmetrically located off the Equator in between the clockwise and counterclockwise circulations. The positive and negative OLR anomalies associated

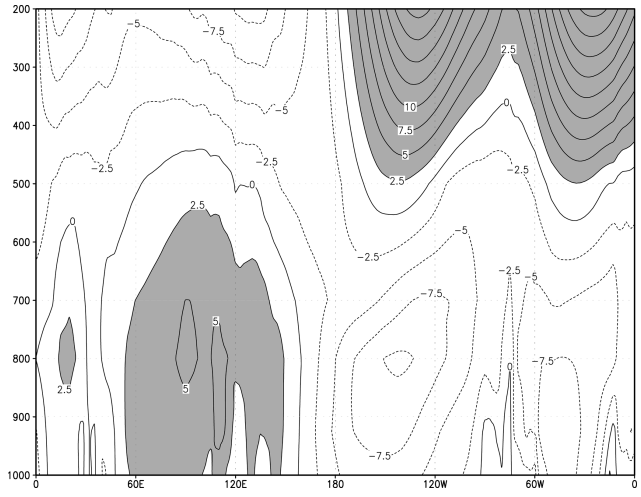

Figure 4. Vertical cross section of the climatological zonal wind ($m\,s^{-1}$) along the Equator between December and February 1991–2020. Shading corresponds to regions of westerlies.

with the MRGW coincide with the regions of convergence and divergence at upper-tropospheric levels. At 500 hPa, the phase of the MRGW over the central Pacific is displaced around 10° to the west with respect to its 200 hPa counterpart (Fig. 2b), reflecting its eastward tilt with height in the troposphere (Suhas et al., 2020). When the signal of the MRGW is calculated at lower-tropospheric levels, a further phase shift towards the west in the clockwise and counterclockwise circulations is observed. At 700 hPa, the intensity of the circulations is weaker than at upper-tropospheric levels, but regions of atmospheric moisture convergence and divergence are observed off the Equator in between the cyclonic and anticyclonic circulations. Just above the tropical boundary layer, the zone of moisture convergence (divergence) is located at 160° W and 5 to 10° S (5 to 10° N) and at around 115° W and 5 to 10° N (5 to 10° S) on the west and east sides of the clockwise circulation in the central Pacific (Fig. 2c). Moisture convergence (divergence) leads to increases (decreases) in atmospheric humidity that tend to coincide with the regions of negative (positive) OLR anomalies. Such connections between upper- and lower-tropospheric levels around the MRGW circulation suggest that tropical convection anomalies are generated at lower-tropospheric levels through moisture convergence that coincide with regions of divergence and convergence at upper-tropospheric levels due to the quadrature in the MRGW between these two tropospheric levels. The phase of the MRGWs tilts eastward with height, from 700 to 200 hPa, i.e., in the troposphere, while the phase tends to tilt westward from the upper troposphere to the lower stratosphere (Holton, 1979; Yang and Hoskins, 2017), reflecting the vertical structure of these equatorial waves.

As an MRGW evolves across the Pacific, the zones of convergence and divergence move westward along with the corresponding convective activity anomalies. The temporal evolution of an MRGW wind field and the associated tropical convection anomalies may be analyzed by examining the sequence of events, from the onset of the equatorial wave around 200 hPa to a few days later, when its signal is observed at lower-tropospheric levels. One-point lag correlations between PC2 and unfiltered anomalies of 200 hPa wind and unfiltered OLR anomalies, for the −2 to +2 d range, show the evolution of an MRGW with an approximate 4 to 5 d period. The vector represents the magnitude of the correlations between PC2 and the zonal and meridional components of the anomalous wind field. At lag −2 d, the correlation with the wind field shows the MRGW pattern over the central eastern Pacific with vortices between 20° N and 20° S. In the central eastern Pacific an anticyclonic equatorial circulation is connected to a midlatitude wave that emanates from the northwest Pacific (Fig. 3a). The cyclonic circulation in midlatitudes mechanically couples with the MRGW that extends across the Pacific, in a similar manner as laterally forced MRGWs presented by Magaña and Yanai (1995), Kiladis et al. (2016), Suhas et al. (2020), and Shreya and Suhas (2024). Over the central Pacific, negative (positive) OLR correlations (anomalies) are observed between the clockwise and counterclockwise circulations of the MRGW over the equatorial region. In the early stages of the MRGW, the OLR anomalies in the central Pacific are modulated by the midlatitude wave train, following the ascending and descending motions described by the omega equation – i.e., negative OLR occurs ahead of troughs. However, at lag 0 d, the MRGW propagates westward along with the antisymmetric anomalies in OLR around the dateline (Fig. 3b), with a westward phase velocity of approximately $15\,m\,s^{-1}$ and a zonal wavenumber 5. The midlatitude wave propagates across the eastern tropical Pacific, extending to the Southern Hemisphere to the western coast of South America (e.g., Braga et al., 2022). At lag +2 d, the regions of convergence and divergence off the Equator, around 15–20° in latitude, are displaced westward along with the tropical convection anomalies of the MRGW (Fig. 3c). At this stage the midlatitude wave train weakens, but the MRGW remains and is present over the westerly duct region, close to the western Pacific.

The maximum amplitude of MRGWs at upper levels occurs over the westerly duct region at 200 hPa, but its amplitude decreases over the western Pacific, i.e., over a region with predominant easterly flow at upper-tropospheric levels (Fig. 4). At lower-tropospheric levels though, the westerly flow is observed over the western Pacific, where MRGWs have been documented at around 850 hPa (Kiladis et al., 2009). In this region, lower-tropospheric MRGWs are better defined and may even lead to the formation of tropical cyclones (Dickinson and Molinari, 2002; Zhou and Wang, 2007).

In the central eastern Pacific, MRGW activity is an important mechanism to modulate the lower-tropospheric moisture

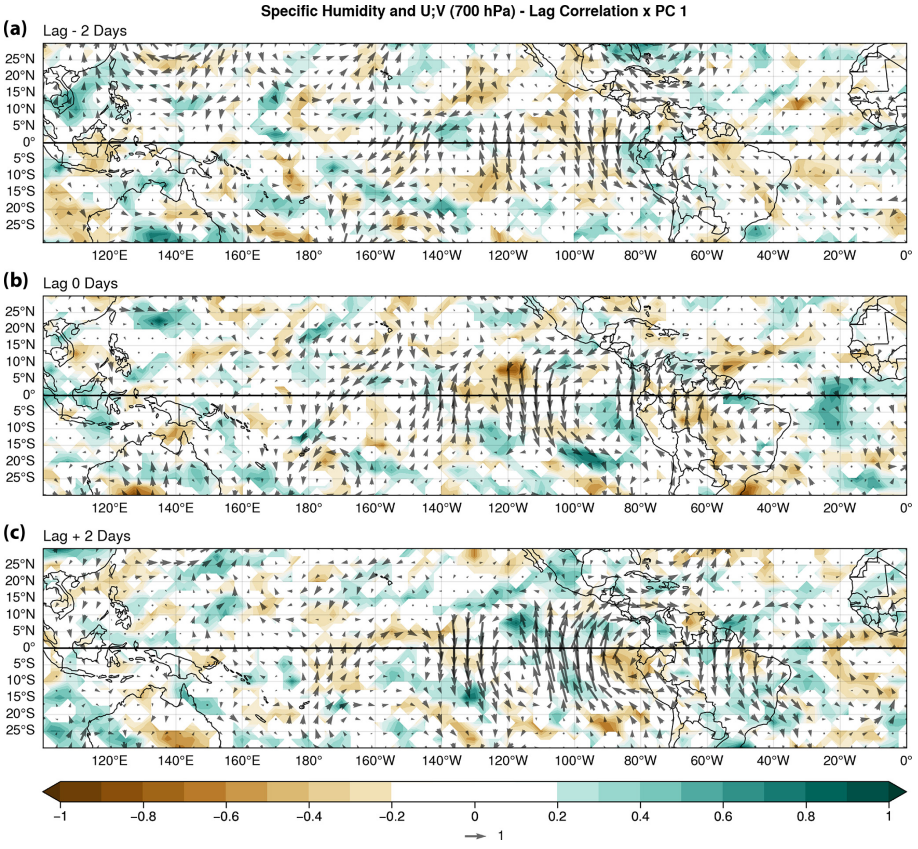

Figure 5. Lagged cross correlation between the first principal component (PC1) and the 700 hPa anomalous wind field (vectors) and 700 hPa specific humidity (shades of green and brown) for the December–February period. Panels show results for **(a)** lag = −2 d, **(b)** lag = 0 d, and **(c)** lag = +2 d. The correlations are calculated with unfiltered anomalies. A vector of magnitude 1 implies a perfect correlation.

field that results in tropical convection. Lagged cross correlations between PC1 and the 700 hPa wind field and anomalies of 700 hPa specific humidity show that MRGWs modulate atmospheric moisture near the boundary layer. At lag −2 d, the clockwise and counterclockwise vortices tend to modulate the antisymmetric response in specific humidity over the eastern Pacific, around 100° W (Fig. 5a). At lag 0 d, the MRGW signal extends from the central Pacific into the western equatorial Atlantic, and the antisymmetric atmospheric moisture anomalies are observed in the corresponding divergent and convergent regions off the Equator, between 5 and 10° in latitude and around 100°–120° W (Fig. 5b). This equatorial disturbance exhibits a dominant zonal wavenumber 5 structure, and its evolution into the Atlantic is in agreement with the eastward group velocity associated with MRGWs. At lag +2 d, the signal for specific humidity correlations moves westward, maintaining the antisymmetric structure off the Equator and extending to the Atlantic Ocean (Fig. 5c). The signal of the MRGW extends to the equatorial Atlantic, and there are some signals of the modulation in the specific humidity field due to the eastward group velocity.

3.2 Vertically integrated moisture flux in the tropics

The modulation of moisture by low-level MRGW circulations is diagnosed by examining the vertically integrated moisture flux (VIMF) and its convergence. As previously stated, VIMF is a measure of the amount of water vapor transported in the atmosphere, and its convergence is used to determine zones of intense convective activity. The lagged correlations of PC1 and VIMF and VIMF convergence show that an MRGW tends to create regions of moisture accumulation that result in tropical convective activity. By lag −2 d, the signals of an MRGW along the eastern equatorial Pacific and a midlatitude wave from the northern subtropics, around the westerly duct region, exhibit the tropical midlatitude interaction signal that leads to the formation of an MRGW (Fig. 6a). The positive and negative vertical motion anomalies are reflected in the regions of VIMF convergence and divergence in the midlatitude wave. In the equatorial region, moisture convergence and divergence are located off the Equator as expected in an MRGW. At lag 0 d, VIMF and its convergence–divergence zones show the westward movement of the MRGW and the antisymmetric location of the associated zones of moisture convergence and divergence

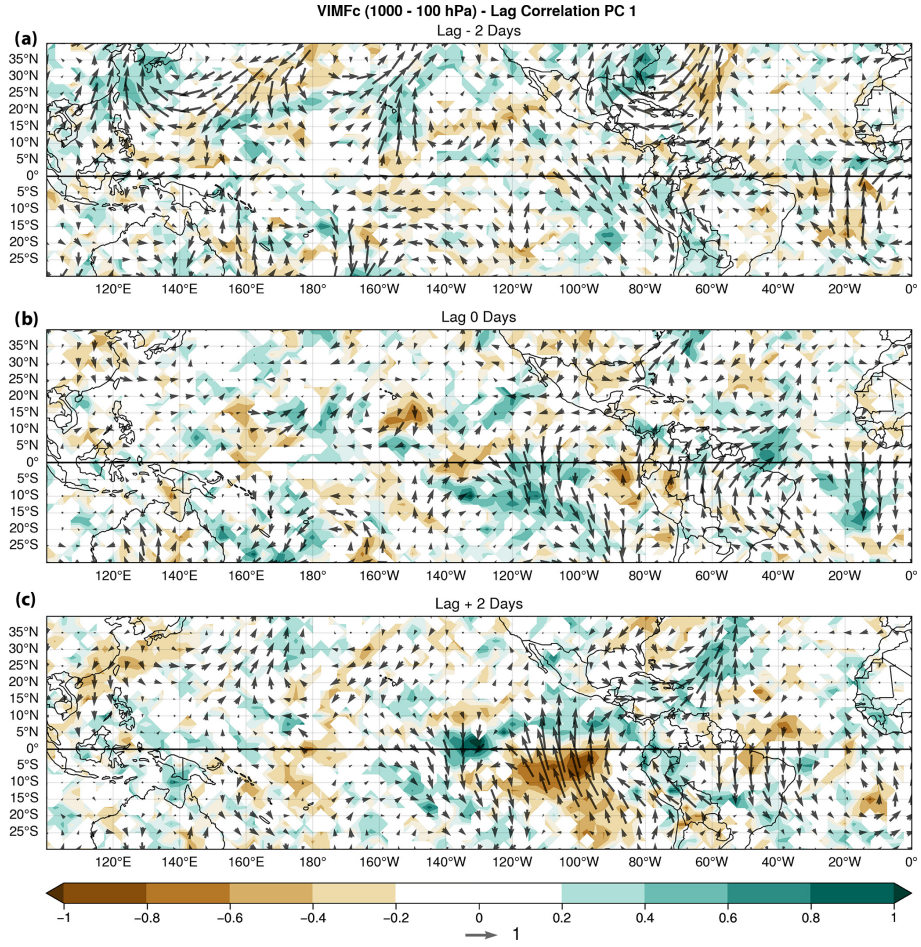

Figure 6. Lagged cross correlation between the first principal component (PC1) and VIMF anomalies (vectors) and VIMF convergence (shades of green) and VIMF divergence (shades of brown) anomalies for the December–February months. **(a)** Lag $= -2$ d, **(b)** lag $= 0$ d, and **(c)** lag $= +2$ d. The correlations are calculated with unfiltered anomalies. A vector of magnitude 1 implies a perfect correlation.

(Fig. 6b). The spatial structure of VIMF correlations approximately matches the one observed for the wind field anomalies at 700 hPa (see Fig. 5b), indicating that VIMF is capturing the signal of MRGWs at lower-tropospheric levels. Such anomalous circulation modulates zones of specific humidity anomalies off the Equator in the central eastern equatorial Pacific. By lag $+2$ d, the MRGW signal shows that moisture convergence and divergence are asymmetrically distributed (Fig. 6c), contributing to increases and decreases in specific humidity between 150 and 70° W. The previous analysis shows that moisture is controlled by the MRGW at lower-tropospheric levels inducing zones of negative and positive convective activity anomalies. The quadrature between the phase of the MRGW at upper- and lower-tropospheric levels serves to connect moisture convergence (divergence) at 700 hPa with divergence (convergence) at 200 hPa, a characteristic of deep tropical convective systems.

The relationship between VIMF convergence–divergence anomalies and OLR anomalies may be shown by means of the lag correlations between PC1 and VIMF convergence and OLR anomalies. For brevity, this relationship is shown only for lag $+2$ d (Fig. 7). The signal of a midlatitude wave approaching the westerly duct region is observed as positive and negative correlations corresponding to VIMF convergence (divergence) and OLR negative (positive) anomalies. Not only does the signal extend into South America, showing that the midlatitude wave triggers an MRGW, but it also continues its interhemispheric propagation (Webster and Holton, 1982; Tomas and Webster, 1994; Li et al., 2015; Kiladis et al., 2016; Braga et al., 2022, 2024). Along the equatorial region the antisymmetric signals in correlation appear for VIMF convergence (divergence) and OLR anomalies extending from 180 to 80° W.

Over the northeastern subtropical Pacific, the interaction between the midlatitude wave and the MRGW VIMF convergence induces a moisture plume that at times results in precipitation events over Mexico (Fig. 7). The structure of such a moisture plume approximately corresponds to the so-called tropical plumes described by Knippertz (2007) and Fröhlich et al. (2013).

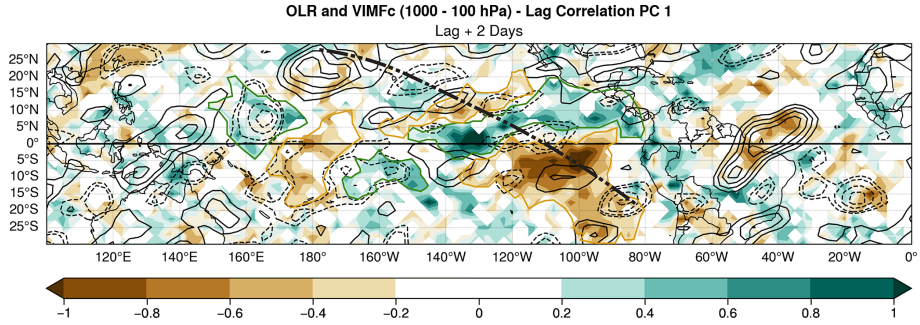

Figure 7. Lagged +2 d correlation between the first principal component (PC1) and OLR and VIMFc unfiltered anomalies. OLR correlations are represented by solid lines (positive) and dashed lines (negative), while VIMF convergence is shown in shades of green and divergence in shades of brown. The thick dashed–dotted line indicates the trajectory of the midlatitude wave. The brown and green lines highlight the zone of antisymmetric VIMFc in the MRGW.

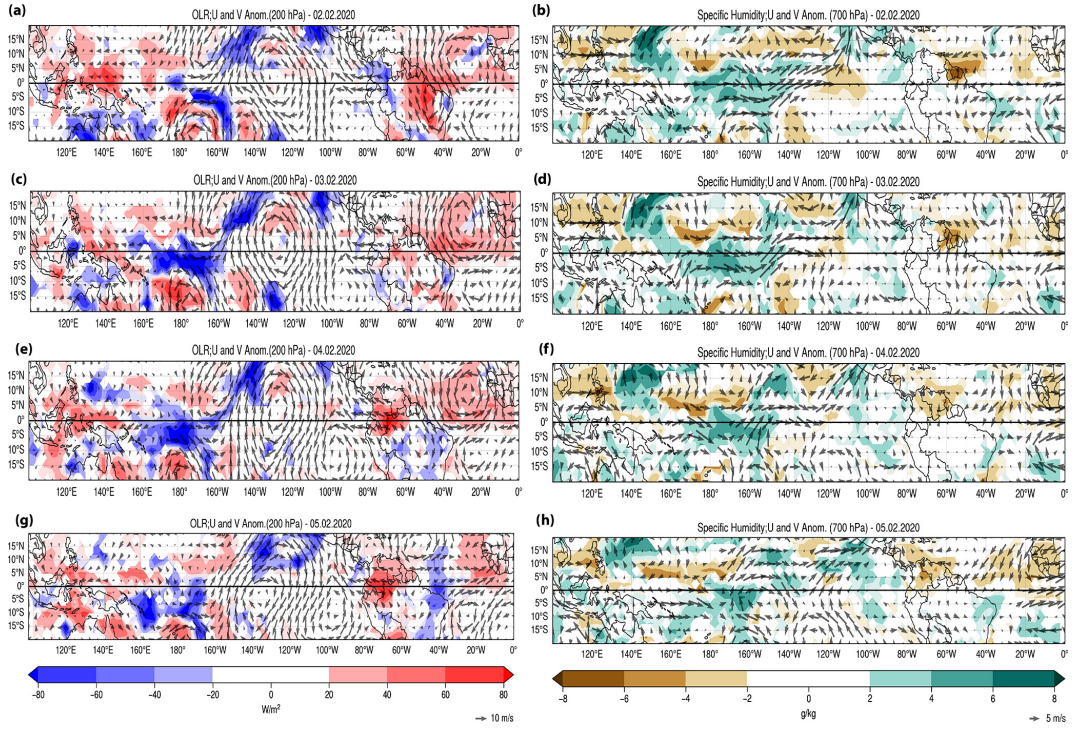

Figure 8. The 200 hPa unfiltered wind anomalies and unfiltered OLR anomalies (left column) and the 700 hPa unfiltered wind field and unfiltered specific humidity anomalies (right column) from 2 to 5 February 2020 for **(a, b)** 2 February, **(c, d)** 3 February, **(e, f)** 4 February, and **(g, h)** 5 February.

3.3 Case study

The presence of MRGWs in the daily atmospheric circulations in upper- and lower-tropospheric levels is obtained for absolute values of PC1 larger than 1.0, like on 2–6 February 2020. On 2 February 2020, a midlatitude wave at upper-tropospheric levels over the central northeastern Pacific propagates into the tropics across the westerly duct region, coupled with the characteristic circulation of an MRGW around 180° W. At 200 hPa (180–120° W) OLR positive and negative anomalies are observed in the regions of ascending and descending motions associated with the midlatitude wave that propagates from the Northern Hemisphere to the Southern Hemisphere (Fig. 8a). The clockwise equatorial circulation at 200 hPa corresponds to part of the midlatitude wave, but it is also a characteristic of the equatorial MRGW. At lower-tropospheric levels (700 hPa), there is only a slight signal of this clockwise circulation, almost in phase with the upper-tropospheric vortex. At this level as well, the midlatitude wave is hardly present in the wind field around the subtropics, but it shows negative and positive specific humidity anomalies in the convergence and divergence regions around

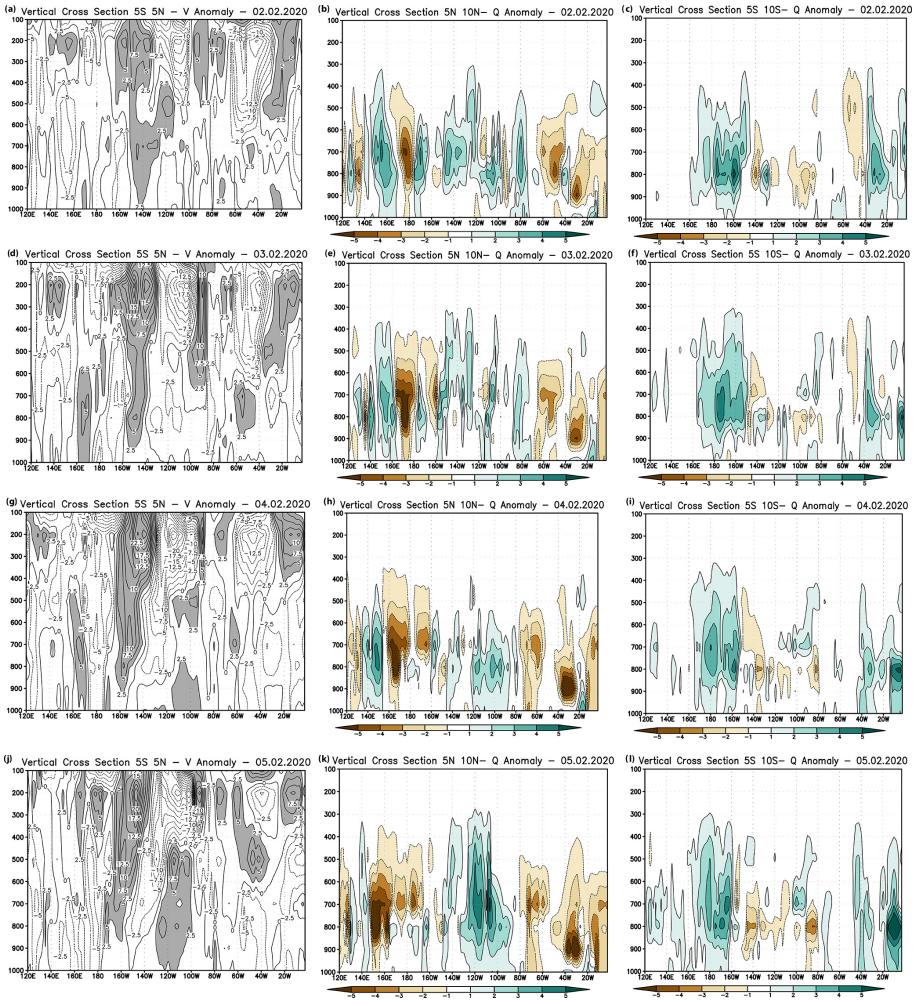

Figure 9. Vertical cross sections (longitude–height) (1000–100 hPa, between 5° S–5° N) for daily unfiltered meridional wind anomalies (left column) and daily unfiltered specific humidity anomalies (central and right columns) from 2 to 5 February 2020: **(a–c)** for 2 February, **(d–f)** for 3 February, **(g–i)** for 4 February, and **(j–l)** for 5 February.

20° N (Fig. 8b). By 3 February 2020, the midlatitude wave at 200 hPa extends to the Pacific coast of South America with the corresponding positive and negative anomalies in OLR (Fig. 8c). At around 130° W, a well-defined vortex corresponds to an equatorial clockwise circulation with antisymmetric OLR anomalies. At 700 hPa, a clockwise circulation may also be identified at 140° W, with signals of a vortex that corresponds to the MRGW with positive and negative specific humidity anomalies around (Fig. 8d). By 4 February 2020, the midlatitude wave in the Northern Hemisphere subtropics remains, but it intensifies in the equatorial and the tropical Southern Hemisphere region (Fig. 8e). In the lower troposphere the clockwise circulation in the equatorial region is better defined and the antisymmetric structure in the surrounding specific humidity anomalies, characteristic of the MRGW, begins to form between 180 and 140° W (Fig. 8f). On 5 February 2020, the MRGW begins its westward movement with antisymmetric OLR anomalies better defined on its westward side. The midlatitude wave signal in the northern central Pacific weakens (Fig. 8g). At lower levels the clockwise circulation associated with the MRGW is well defined over the Equator and shows a westward displacement with the specific humidity anomalies antisymmetrically distributed around this circulation in the moisture convergent and divergent regions (Fig. 8h). The structure of the MRGW at 700 hPa appears to be better defined as it approaches the westerly winds, west of the dateline.

As observed by Zhou and Wang (2007) in their case study, an MRGW is triggered at upper-tropospheric levels, and its signal propagates downward in the following days. The sequence of atmospheric circulations between 2–5 February 2020 shows that the equatorial wave circulations are well defined in the early days at 200 hPa, and its presence is better detected at later stages at 700 hPa. A vertical cross section of the meridional wind anomalies along the Equator and specific humidity anomalies north and south of the Equa-

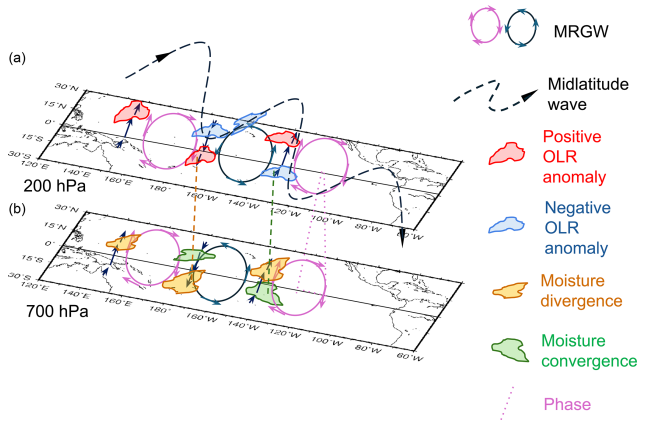

Figure 10. Schematic representation of the vertical structure of an MRGW and the corresponding circulation anomalies in the lower-tropospheric **(a)** and upper-tropospheric **(b)** levels along with moisture and convective activity anomalies in divergent and convergent regions (vectors) of the wave. The dashed wavy line corresponds to the midlatitude wave in the upper troposphere.

tor (5° N–5° S) reflect the development of the vertical structure of the MRGW. The vertical cross section of the meridional wind anomalies between 5° S and 5° N (Fig. 9a) and specific humidity anomalies between 5 and 10° S (Fig. 9b) and 5 and 10° N (Fig. 9c) for 2 February 2020 shows that the signal of the MRGW in the wind field is present mainly at 200 hPa around 160–100° W with a magnitude of around 15 m s^{-1} between 100 and 400 hPa. At this stage of development, the specific humidity anomalies do not appear to correspond to the moisture convergence and divergence induced by an MRGW. By 3 February 2020, the signal of the MRGW in the central eastern Pacific, at upper-tropospheric levels, extends downward to around 700 hPa (Fig. 9d). Some indications of the induced effect of the lower-tropospheric part of the MRGW are found in the specific humidity, with positive–negative anomalies around 700 hPa between 160° E and 140° W (Fig. 9e). South of the Equator the sign of these anomalies tends to be the opposite to its northward counterpart, but it is still not well defined (Fig. 9f). By 4 February 2020, the quadrature in the anomalies of the meridional component of the wind field shows and extends to lower-tropospheric levels with an eastward tilt with height at around 150° W (Fig. 9g). The tilt with height approximately corresponds to a vertical wavelength of around 15 km, which approximately agrees with early estimates by Yanai and Hayashi (1969). At around 700 hPa positive and negative anomalies appear to be induced by moisture convergence and divergence associated with the MRGW (Fig. 9h and i). On 5 February 2020, the structure of the MRGW in the troposphere exhibits the tilt with height associated with the vertical wavelength between 180 and 120° W (Fig. 9j). North and south of the Equator, antisymmetric anomalies in the specific humidity field are well defined in association with the circulations induced by the MRGW (Fig. 9k and l). This case study suggests that the moisture anomalies in the lower-tropospheric levels tend to develop as the MRGW propagates downward from the upper-tropospheric levels where it was triggered by a midlatitude wave. Once the MRGW is well developed, it modulates moisture convergence and develops as deep convection due to the wind divergence in the upper troposphere.

These results are like those of Zhou and Wang (2007) and indicate a change in the wavelength of the MRGW as the signal propagates from the upper-tropospheric levels over the western Pacific. As the MRGW signal propagates downward and westward into the western Pacific, the wavelength appears to decrease from a dominant wavenumber 5 to a zonal wavenumber 6. The change from easterlies to westerlies appears to affect the propagation and energetics of the MRGW at lower-tropospheric levels (Webster and Chang, 1988) and may influence the change in the spatial structure of the MRGW at lower-tropospheric levels.

4 Summary and conclusions

Upon the discovery of equatorial waves, numerous studies have proposed that they are forced either by a midlatitude wave propagating into the tropics or by convective activity near the equatorial regions. Lateral forcing appears to be the most frequently accepted triggering mechanism for MRGWs (Magaña and Yanai, 1995; Zhou and Wang, 2007; Suhas et al., 2020; Shreya and Suhas, 2024). However, there is still some debate on the relationship between MRGWs and tropical convective activity. Moreover, the signals of MRGWs in the upper and lower troposphere are often treated separately.

The present study shows a plausible explanation to coherently relate all these elements considering forcing of equatorial circulation with the characteristics of an MRGW by a midlatitude wave that propagates across the westerly duct region. As suggested by Au-Yeung and Tam (2018), the MRGW extends from the upper-tropospheric level, where it is initiated, to the lower-tropospheric level, where it changes the atmospheric moisture field, resulting in antisymmetric anomalies in specific humidity off the Equator, like those reported in other observational analyses (e.g., Kiladis et al., 2009). The phase difference (quadrature) between the upper-tropospheric MRGW circulations (wind convergence–divergence) and its lower-tropospheric counterpart (moisture divergence–convergence) reinforces the development of deep tropical convection that shows as positive and negative OLR anomalies off the Equator (Fig. 10). Therefore, a key element to associate convective activity and atmospheric circulation in an MRGW is the eastward tilt with height in the troposphere that results in a quadrature of the phase of the wave. From the top of the troposphere to the stratosphere the westward tilt with height corresponds to the vertical structure of the MRGW (e.g., Holton, 1979; Yang and Hoskins, 2017).

The development of MRGWs constitutes a process that involves tropical midlatitude interactions that are of relevance for weather in the tropical region, where moisture convergence in the eastern tropical Pacific induced by MRGWs constitutes the source of convective activity, even for tropical plumes observed over Mexico during the boreal winter season (Knippertz, 2007; Fröhlich et al., 2013). In addition, the propagation of the midlatitude wave into the Southern Hemisphere through the westerly duct affects weather over South America (Braga et al., 2022).

Thanks to the improvement in atmospheric reanalysis, it is now possible to more accurately describe the characteristics of equatorial waves in the troposphere and even in the stratosphere. A systematic identification of equatorial wave activity may serve to better define the influence of these systems on weather in several tropical regions, for instance in the tropical Americas. In summary, a key element of tropical weather in the eastern Pacific is MRGWs, and consequently, a better understanding of the processes of modulation of atmospheric moisture and convective activity may significantly improve weather forecasts in the tropical and subtropical regions.

Data availability. Publicly available datasets were analyzed in this study. These data can be found here: https://www.ecmwf.int/en/forecasts/dataset/ecmwf-reanalysis-v5 (ECMWF, 2024).

Author contributions. HAB analyzed the data, wrote the manuscript, and prepared the figures. VM contributed some parts and reviewed the manuscript together with the first author.

Competing interests. The contact author has declared that neither of the authors has any competing interests.

Disclaimer. Publisher's note: Copernicus Publications remains neutral with regard to jurisdictional claims made in the text, published maps, institutional affiliations, or any other geographical representation in this paper. While Copernicus Publications makes every effort to include appropriate place names, the final responsibility lies with the authors.

Acknowledgements. We are grateful to the Departamento de Geografia Física at the Instituto de Geografía, UNAM, for their valuable support. We especially thank Gustavo Vázquez for his outstanding technical assistance. This project was made possible through a DGAPA-UNAM postdoctoral fellowship (grant no. 13189) and the CONAHCYT grant (grant no. PCC-319779). We sincerely thank George Kiladis and the anonymous reviewer for their constructive comments and suggestions, which have significantly improved the manuscript.

Financial support. This work was supported by UNAM Postdoctoral Program (POSDOC – DGAPA 13189) and by CONAHCYT grant PCC-319779.

Review statement. This paper was edited by Peter Knippertz and reviewed by George Kiladis and one anonymous referee.

References

Au-Yeung, A. Y. M. and Tam, C.-Y.: Dispersion characteristics and circulation associated with boreal summer westward-traveling mixed Rossby–gravity wave–like disturbances, J. Atmos. Sci., 75, 513–533, https://doi.org/10.1175/JAS-D-16-0245.1, 2018.

Bennet, J. R. and Young, J. A.: The influence of latitudinal with shear upon large-scale wave propagation into the tropics, Mon. Weather Rev., 99, 201–214, https://doi.org/10.2151/jmsj1965.52.3_261, 1971.

Braga, H. A., Ambrizzi, T., and Hall, N. M. J.: Relationship between interhemispheric Rossby wave propagation and South Atlantic Convergence Zone during La Niña years, Int. J. Climatol., 13, 8652–8664, https://doi.org/10.1002/joc.7755, 2022.

Braga, H. A., Ambrizzi, T., and Hall, N. M. J.: South Atlantic Convergence Zone as Rossby wave source, Theor. Appl. Climatol., 155, 4231–4247, https://doi.org/10.1007/s00704-024-04877-y, 2024.

Dickinson, M. and Molinari, J.: Mixed Rossby–Gravity Waves and Western Pacific Tropical Cyclogenesis. Part I: Synoptic Evolution, J. Atmos. Sci., 59, 2183–2196, https://doi.org/10.1175/1520-0469(2002)059<2183>2.0.CO;2, 2002.

Duchon, C. E.: Lanczos filtering in one and two dimensions, J. Appl. Meteor. Climatol., 18, 1016–1022, https://doi.org/10.1175/1520-0450(1979)018<1016>2.0.CO;2, 1979.

ECMWF: ECMWF Reanalysis v5 (ERA5), Copernicus [data set], https://www.ecmwf.int/en/forecasts/dataset/ecmwf-reanalysis-v5 (last access: September 2024), 2024.

Fasullo, J. and Webster, P. J.: A hydrological definition of Indian monsoon onset and withdrawal, J. Climate, 16, 3200–3211, https://doi.org/10.1175/1520-0442(2003)016<3200>2.0.CO;2, 2003.

Fröhlich, L., Knippertz, P., Fink, A. H., and Hohberger, E.: An objective climatology of tropical plumes, J. Climate, 26, 5044–5060, https://doi.org/10.1175/JCLI-D-12-00351.1, 2013.

Hayashi, Y.: A theory of large-scale equatorial waves generated by condensation heat and accelerating, J. Meteor. Soc. Jpn. Ser. II, 48, 140–160, https://doi.org/10.2151/jmsj1965.48.2_140, 1970.

Hayashi, Y.: Interpretations of space-time spectral energy equations, J. Atmos. Sci., 39, 685–688, https://doi.org/10.1175/1520-0469(1982)039<0685>2.0.CO;2, 1982.

Hayashi, Y. and Golder, D. G.: The generation of equatorial transient planetary waves: Control experiments with a GFDL general circulation model, J. Atmos. Sci., 35, 2068–2082, https://doi.org/10.1175/1520-0469(1978)035<2068>2.0.CO;2, 1978.

Hess, P., Hendon, H., and Battisti, D. S.: The relationship between mixed Rossby gravity waves and convection in a general circulation model, J. Meteor. Soc. Jpn., 71, 321–338, 1993.

Hersbach, H., Bell, B., Berrisford, P., Hirahara, S., Horányi, A., Muñoz-Sabater, J., Nicolas, J., Peubey, C., Radu, R., Schepers, D., Simmons, A., Soci, C., Abdalla, S., Abellan, X., Balsamo, G., Bechtold, P., Biavati, G., Bidlot, J., Bonavita, M., Chiara, G., Dahlgren, P., Dee, D., Diamantakis, M., Dragani, R., Flemming, J., Forbes, R., Fuentes, M., Geer, A., Haimberger, L., Healy, S., Hogan, R. J., Hólm, E., Janisková, M., Keeley, S., Laloyaux, P., Lopez, P., Lupu, C., Radnoti, G., Rosnay, P., Rozum, I., Vamborg, F., Villaume, S., and Thépaut, J.-N.: The ERA5 global reanalysis, Q. J. Roy. Meteorol. Soc., 146, 1999–2049, https://doi.org/10.1002/qj.3803, 2020.

Holton, J. R.: Waves in the equatorial stratosphere generated by tropospheric heat sources, J. Atmos. Sci., 29, 368–375, https://doi.org/10.1175/1520-0469(1972)029<0368>2.0.CO;2, 1972.

Holton, J. R.: An Introduction to Dynamic Meteorology, Academic Press, New York, San Francisco, London, 391 pp., ISBN 0123848660, 1979.

Kiladis, G. N., Wheeler, M. C., Haertel, P. T., Straub, K. H., and Roundy, P. E.: Convectively coupled equatorial waves, Rev. Geophys., 47, RG2003, https://doi.org/10.1029/2008RG000266, 2009.

Kiladis, G. N., Dias, J., and Gehne, M.: The relationship between equatorial mixed Rossby–gravity and eastward inertio-gravity waves. Part I, J. Atmos. Sci., 73, 2123–2145, https://doi.org/10.1175/JAS-D-15-0230.1, 2016.

Knippertz, P.: Tropical–extratropical interactions related to upper-level troughs at low latitudes, Dyn. Atmos. Oceans, 43, 36–62, https://doi.org/10.1016/j.dynatmoce.2006.06.003, 2007.

Knippertz, P., Gehne, M., Kiladis, G. N., Kikuchi, K., Rasheeda Satheesh, A., Roundy, P. E., Yang, G., Žagar, N., Dias, J. Fink, A. H.,, Methven, J., Schlueter, A., Sielmann, F., and Wheeler, M. C.: The intricacies of identifying equatorial waves, Q. J. Roy. Meteorol. Soc., 148, 2814–2852, https://doi.org/10.1002/qj.4338, 2022.

Li, Y., Li, J., Jin, F. F., and Zhao. S: Interhemispheric propagation of stationary Rossby waves in a horizontally nonuniform background flow, J. Atmos. Sci., 72, 3233–3256, https://doi.org/10.1175/JAS-D-14-0239.1, 2015.

Liebmann, B. and Smith, C. A.: Description of a complete (interpolated) outgoing longwave radiation dataset, B. Am. Meteor. Soc., 77, 1275–1277, https://doi.org/10.2307/26233278, 1996.

Magaña, V. and Yanai, M.: Tropical-midlatitude interaction on the time scale of 30 to 60 days during the Northern summer of 1979, J. Climate, 4, 180–201, https://doi.org/10.1175/1520-0442(1991)004<0180>2.0.CO;2, 1991.

Magaña, V. and Yanai, M.: Mixed Rossby–gravity waves triggered by lateral forcing, J. Atmos. Sci., 52, 1473–1486, https://doi.org/10.1175/1520-0469(1995)052<1473>2.0.CO;2, 1995.

Mak, M.: Laterally driven stochastic motions in the tropics, J. Atmos. Sci., 26, 41–64, https://doi.org/10.1175/1520-0469(1969)026<0041>2.0.CO;2, 1969.

Maruyama, T.: Large-scale disturbances in the equatorial lower stratosphere, J. Meteor. Soc. Jpn. Ser. II, 45, 391–408, https://doi.org/10.2151/jmsj1965.45.5_391, 1967.

Matsuno, T.: Quasi-geostrophic motions in the equatorial area, J. Meteor. Soc. Jpn. Ser. II, 44, 25–43, https://doi.org/10.2151/jmsj1965.44.1_25, 1966.

Nitta, T.: Statistical study of tropospheric wave disturbances in the tropical Pacific region, J. Meteor. Soc. Jpn. Ser. II, 48, 47–60, https://doi.org/10.2151/jmsj1965.48.1_47, 1970.

Pazos, M., Magaña, V., and Herrera, E.: Easterly wave activity in the Intra-Americas Seas region analyzed with vertically integrated moisture fluxes, Front. Earth Sci., 11, 1223939, https://doi.org/10.3389/feart.2023.1223939, 2023.

Suhas, E., Neena, J. M., and Jiang, X.: Exploring the factors influencing the strength and variability of convectively coupled mixed Rossby–gravity waves, J. Climate, 33, 9705–9719, https://doi.org/10.1175/JCLI-D-20-0218.1, 2020.

Shreya, K. and Suhas, E.: A survey of westward-propagating mixed Rossby–Gravity waves and quantification of their association with extratropical disturbances, Q. J. Roy. Meteorol. Soc., 150, 1752–1770, https://doi.org/10.1002/qj.4668, 2024.

Takayabu, N. Y. and Nitta, T.: 3–5 day-period disturbances coupled with convection over the tropical Pacific Ocean, J. Meteor. Soc. Jpn., 71, 221–245, https://doi.org/10.2151/jmsj1965.71.2_221, 1993.

Tomas, R. A. and Webster, P. J.: Horizontal and vertical structure of cross-equatorial wave propagation, J. Atmos. Sci., 51, 1417–1430, https://doi.org/10.1175/1520-0469(1994)051<1417>2.0.CO;2, 1994.

Webster, P. J. and Chang, H.: Equatorial energy accumulation and emanation regions: Impacts of a zonally varying basic state, J. Atmos. Sci., 45, 803–829, https://doi.org/10.1175/1520-0469(1988)045<0803:EEAAER>2.0.CO;2, 1988.

Webster, P. J. and Holton, J. R.: Cross-equatorial response to middle-latitude forcing in a zonally varying basic state, J. Atmos. Sci., 39, 722–733, https://doi.org/10.1175/1520-0469(1982)039<0722>2.0.CO;2, 1982.

Wheeler, M. and Kiladis, G. N.: Convectively coupled equatorial waves: Analysis of clouds and temperature in the wavenumber–frequency domain, J. Atmos. Sci., 56, 374–399, https://doi.org/10.1175/1520-0469(1999)056<0374>2.0.CO;2, 1999.

Yanai, M. and Hayashi, Y.: Large-scale equatorial waves penetrating from the upper troposphere into the lower stratosphere, J. Meteor. Soc. Jpn. Ser. II, 47, 167–182, https://doi.org/10.2151/jmsj1965.47.3_167, 1969.

Yanai, M. and Lu, M.: Equatorially trapped waves at the 200 mb level and their association with meridional convergence of wave energy flux, J. Atmos. Sci., 40, 2785–2803, https://doi.org/10.1175/1520-0469(1983)040<2785>2.0.CO;2, 1983.

Yanai, M. and Maruyama, T.: Stratospheric wave disturbances propagating over the equatorial Pacific, J. Meteor. Soc. Jpn. Ser. II, 44, 291–294, https://doi.org/10.2151/jmsj1965.44.5_291, 1966.

Yanai, M. and Murakami, M.: A further study of tropical wave disturbances by the use of spectrum analysis, J. Meteor. Soc. Jpn. Ser. II, 48, 185–197, https://doi.org/10.2151/jmsj1965.48.3_185, 1970a.

Yanai, M. and Murakami, M.: Spectrum analysis of symmetric and antisymmetric equatorial waves, J. Meteor. Soc. Jpn. Ser. II, 48, 331–347, https://doi.org/10.2151/jmsj1965.48.4331, 1970b.

Yang, G. and Hoskins, B. J.: The equivalent barotropic structure of waves in the tropical atmosphere in the Western Hemisphere, J. Atmos. Sci., 74, 1689–1704, https://doi.org/10.1175/JAS-D-16-0267.1, 2017.

Yang, G., Hoskins, B., and Slingo, J.: Convectively coupled equatorial waves: A new methodology for identifying wave structures in observational data, J. Atmos. Sci., 60, 1637–1654, https://doi.org/10.1175/1520-0469(2003)060<1637>2.0.CO;2, 2003.

Yang, G., Methven, J., Woolnough, S., Hodges, K., and Hoskins, B.: Linking African easterly wave activity with equatorial waves and the influence of Rossby waves from the Southern Hemisphere, J. Atmos. Sci., 75, 1783–1809, https://doi.org/10.1175/JAS-D-17-0184.1, 2018.

Yang, G.-Y. and Hoskins, B. J.: ENSO-related variation of equatorial MRG and Rossby waves and forcing from higher latitudes, Q. J. Roy. Meteorol. Soc., 142, 2488–2504, https://doi.org/10.1002/qj.2842, 2016.

Zhang, C. and Webster, P. J.: Laterally forced equatorial perturbations in a linear model. Part I: Stationary transient forcing, J. Atmos. Sci., 49, 585–607, https://doi.org/10.1175/1520-0469(1992)049<0585>2.0.CO;2, 1992.

Zhou, X. and Wang, B.: Transition from an eastern Pacific upper-level mixed Rossby-gravity wave to a western Pacific tropical cyclone, Geophys. Res. Lett., 34, L24801, https://doi.org/10.1029/2007GL031831, 2007.